

Contents list available at CBIORE journal website

International Journal of Renewable Energy Development

Journal homepage: https://ijred.cbiore.id



Research Article

Parametric study on the hydrothermal synthesis of fluorescent p-doped carbon quantum dots from banana peels (*Musa acuminata*) and their photocatalytic performance towards hexavalent chromium reduction

Christian M. Claus* , Monet Concepcion M. Detras* , Jewel A. Capunitan , Rowena B. Carpio , Marilyn C. del Barrio

Department of Chemical Engineering, College of Engineering and Agro-Industrial Technology, University of the Philippines Los Baños, College, Los Baños, Laguna, 4031, Philippines

Abstract. Hexavalent chromium (Cr(VI)) represents a significant risk to both human health and the environment. Photocatalysis offers a promising method for reducing Cr(VI) to the less toxic Cr(III) state, which can be easily precipitated and removed. Carbon quantum dots (CQDs) have become prominent in photocatalysis owing to their facile synthesis, light-harvesting capacity, and electron transfer properties. In this study, banana peel (Musa acuminata) powder containing approximately $59.58 \pm 7.43\%$ (w/w) carbohydrates and $15.67 \pm 0.15\%$ (w/w) moisture, serves as a sustainable carbon source for synthesizing CQDs, through the hydrothermal method. Phosphoric acid was introduced as a dopant and catalyst, promoting the formation of fluorescent phosphorus-doped carbon quantum dots (P-CQDs). These P-CQDs were then used as photocatalysts for the visible light-induced reduction of Cr(VI). This research employed a 2^k factorial experimental design to evaluate the effects of hydrothermal synthesis conditions such as phosphoric acid-to-banana peel powder mass ratio (1:1 to 2:1), reaction temperature (140°C to 180°C), and reaction time (4 to 8 hours) on the photoreduction of 50ppm Cr(VI) in synthetic wastewater. Photoreduction efficiencies ranged from 57.3% to 85.4% after 2 hours of visible light irradiation. Analysis of Variance (ANOVA) results at a 95% confidence interval demonstrated that all three factors significantly influenced the reduction efficiency. Furthermore, UV-Vis spectroscopy of P-CQDs at varying hydrothermal synthesis conditions revealed characteristic absorption bands at π - π * transitions of the C=C bonds in the core structure and n- π * transitions of C=O/P domains on the surface. Meanwhile, FTIR analysis of P-CQD samples has shown several peaks corresponding to hydroxyl, carbonyl, carbonyl, and phosphorus-containing functional groups. The synthesized compound also exhibited strong photoluminescence with blue-green emission under 365 nm UV light. These findings are crucial for further research ai

Keywords: Carbon quantum dots, p-doped, banana peels, phosphoric acid, photocatalysis, hexavalent chromium



@ The author(s). Published by CBIORE. This is an open access article under the CC BY-SA license (http://creativecommons.org/licenses/by-sa/4.0/).

Received: 17th May 2025; Revised: 16th July 2025; Accepted: 17th August 2025; Available online: 31st August 2025

1. Introduction

The widespread distribution of heavy metals in aquatic ecosystems, driven by natural factors and diverse industrial applications, has sparked significant environmental concerns due to their potential threats to ecological systems and human well-being (Tchounwou *et al.*, 2012; Sa'adah *et al.*, 2024)). Among these metals, chromium is particularly concerning due to its wide usage in industrial operations such as textile dyeing (Cetin *et al.*, 2008), metal plating (Kropschot & Doebrich, 2010), pigment making (Burstein *et al.*, 2010), ceramic manufacturing (Wilbur *et al.*, 2012), electroplating (Yli-Pentti *et al.*, 2014), and leather tanning (Omm-e-Hany *et al.*, 2018).

Cr(0), Cr(III), and Cr(VI) are the most prevalent oxidation states of chromium. Among these, hexavalent chromium (Cr(VI)) is the most hazardous owing to its strong oxidizing nature and high mobility in biological systems (Marqués *et al.*, 1998). The International Agency for Research on Cancer (IARC)

classifies Cr(VI) as a Group 1 human carcinogen, with exposure linked to severe health effects, including organ damage and death at high doses (ATSDR, 2000). Therefore, reducing Cr(VI) to its less harmful trivalent state Cr(III) is critically important.

Widely studied methods for treating chromium-containing wastewater, such as electrocoagulation, chemical coagulation and flocculation, adsorption, and membrane techniques, often generate toxic secondary waste and can be costly (Teh *et al.*, 2016; Sukmana *et al.*, 2021). Photocatalysis has emerged as a promising alternative, with various photocatalysts being developed to enhance the process. However, metal oxide photocatalysts like ZnO, Zeolites, and TiO_2 although effective, can be toxic (Peralta-Videa *et al.*, 2011) and typically active only under ultraviolet (UV) light which is impractical for most applications (Shen *et al.*, 2013). This has led to increased research into visible-light-absorbing photocatalysts.

Carbon quantum dots (CQDs), with excellent lightharvesting capabilities, electron transfer properties, and

^{*} Corresponding author Email: cmclaus@up.edu.ph (C.M. Claus)

environmental friendliness, are appealing options (Das *et al.*, 2021; Alkian *et al.* 2022). These quasi-zero dimensional nanoparticles, typically smaller than 10nm in diameter, consist of an sp² carbon core with diverse surface moieties (Xia *et al.*, 2019). CQDs are valued for their facile synthesis, cost-effectiveness, photoluminescence, UV-vis absorption, tunable energy band gap, biocompatibility, and nontoxicity (Jiang *et al.*, 2019; Kailasa *et al.*, 2019; Tungare *et al.*, 2020).

Methods for synthesizing CQDs are generally divided into into top-down and bottom-up routes. In the top-down method, larger carbon-based materials are fragmented into nanosized particles through ultrasonication, laser ablation, electrochemical, or chemical oxidative process (Carbonaro et al., 2019). However, these methods often suffer from low yield and high cost (John et al., 2021; Hoang et al., 2023). A promising alternative is the bottom-up approach, particularly hydrothermal synthesis, which builds CQDs by gradual assembly of atoms or molecules (Cai et al., 2019). This method is favored due to its low cost nature, eco-friendly characteristics, and the ease of introducing heteroatom dopant into the organic precursors (Wang et al., 2021; Ramar et al., 2019; Kalaiyarasan et al., 2020).

The synthesis of CQDs can utilize a range of precursor materials, categorized as either chemical or green sources (Omar et al., 2022). Recently, there has been a surge of attention in utilizing sustainable green precursors like fruit peels (Muktha et al., 2020; Atchudan et al., 2021) due to their abundance and environmental benefits. For instance, banana peels, which constitute 40% to 50% of the ripe fruit (Ahmed et al., 2021), are often discarded as waste despite containing valuable components like cellulose, hemicellulose, pectin, lignin, and other carbon-rich organic compounds (Alzate-Acevedo et al., 2021). The Philippines, a major banana producer and the top exporter in Asia generated an estimated 2.36 million metric tons of bananas from July to September 2022, leading to substantial amounts of peel waste (DA, 2022; FAO UN, 2022). If not properly managed, these peels can decompose for up to two years, emitting greenhouse gases and contributing to climate change (Alzate-Acevedo et al., 2021).

Given the organic content of banana peels, they present as a viable green precursor for producing CQDs. Although previous studies have explored banana peels as a carbon feedstock for producing CQDs (Vikneswaran et al., 2014; Atchudan et al., 2020), the applications of their phosphorus-doped form remains largely unexplored. Doping CQDs with heteroatoms like phosphorus can enhance fluorescence, significantly alter their energy band structure, and modify their surface chemistry, leading to improved catalytic performance (Zhang et al., 2020). In this study, phosphoric acid is used as a dopant for its environmental benignity and potential to fine-tune the properties of CQDs (Quesada-Plata et al., 2016), offering a sustainable approach to chromium pollution mitigation. Furthermore, the synthesis of P-CQD photocatalysts that are active under visible light opens new opportunities for their use in sunlight-driven water treatment and in the development of solar energy technologies, given that ultraviolet light accounts for only about 7% of sunlight, while the majority lies in the visible spectrum (Akbar et al., 2021).

2. Materials and Method

2.1 Chemicals and Materials

Reagents such as phosphoric acid (85 - 88%, Ajax Finechem), potassium dichromate (99.98%, Loba Chemie), sodium



Fig. 1 P-CQD Synthesis Schematic Diagram

hydroxide (\geq 98%, RCI Labscan), 1,5-diphenylcarbazide (\geq 95%, Sigma-Aldrich), acetone (\geq 99.5%, JT Baker) and deionized water (0.5 μ S/cm) were sourced from local suppliers and used as received without further treatment. Teflon-lined hydrothermal reactor (250ml), visible light lamp (36W fluorescent lamp with electronic ballast), UV light (365nm), glass microfiber filter (1.2 μ m, Whatman), and mixed-cellulose ester (MCE) membrane filter (0.22 μ m, Scharlau) were also obtained commercially.

2.2 Banana Peels Pretreatment and Characterization

Banana fruit and peels (*Musa acuminata*) from this study were obtained from different supermarkets in Muntinlupa and Las Piñas City, Philippines. The peels and pulp of the fruit were separated. The collected peels were thouroughly washed, chopped into smaller pieces, and oven-dried at 105∘C for 8 hours. Afterwards, they were pulverized into a fine powder using a commercially available blender. The banana peel powder (BPP) underwent sieving using a standard sieve no. 60 (≤ 250 microns) to ensure uniformity of size. Proximate analysis was conducted to determine the carbohydrate, protein, lipids, ash, and moisture content of the powdered dry banana peels. Fourier Transform Infrared Spectroscopy (FTIR) with Attenuated Total Reflection (Shimadzu, IR Tracer-100) was also employed to determine the surface-bound functional groups on the BPP.

2.3 Hydrothermal Synthesis and Purification of P-CQDs

About 12.0g of dried banana peel powder (BPP) and varying amounts of phosphoric acid, H_3PO_4 (12.0g to 24.0g) were soaked in 60 mL of deionized water for 14h (Liu *et al.*, 2021, Goswami *et al.*, 2022). The mixture was placed into a Teflon-lined hydrothermal reactor (Figure 1) and subjected to heating in a laboratory oven at different temperatures (140°C to 180°C) and reaction times (4h to 8h). Subsequently, the product thus acquired from hydrothermal synthesis was cooled to room temperature and filtered using a glass microfiber filter (1.2 μ m). The supernatant solution underwent another filtration step using a MCE membrane filter. (Atchudan *et al.*, 2020).

2.4 Photocatalytic Reduction Experiment

A 1ml of the P-CQD solution was added to a synthetic 50ppm of hexavalent chromium solution. The acidic requirement of the reduction (pH \approx 2) was achieved using 0.1M NaOH (Shen *et al.*, 2013). The beaker containing hexavalent chromium and P-CQDs was subsequently preset for 30 minutes (Xu *et al.*, 2018). It was mixed thoroughly with a magnetic stirrer and then irradiated for 2 hours with a 36W fluorescent lamp (with electronic ballast) at a 20cm vertical distance from the surface of the medium (Rahim *et al.*, 2012).

Table 1Summary of Factorial Levels of the Experiment

Factor	Low Level	High Level	
[A] H ₃ PO ₄ : BPP Mass Ratio	1	2	
[B] Reaction Temperature (°C)	140	180	
[C] Reaction Time (h)	4	8	

Meanwhile, the hexavalent chromium in this study was measured using the procedure specified in the Standard Methods for the Examination of Water and Wastewater (Baird & Bridgewater, 2017). The initial and final concentration of hexavalent chromium was examined in the UV-Vis Spectroscope at 540nm using diphenylcarbazide (DPC) assay.

2.5 Statistics and Experimental Design

The effect of phosphoric acid: banana peel powder mass ratio [A], reaction temperature [B], and reaction time [C] on the photoreduction efficiency of 50 ppm Cr(VI) under 2 hrs visible light irradiation was evaluated by performing a 2^k factorial experiment with Analysis of Variance (ANOVA) at 95% confidence interval using Design Expert 11. The levels of the factors used can be found in Table 1.

2.6 Characterization of P-CQDs

Absorption peaks and optical characteristics of the synthesized compound were analyzed using UV-vis Spectroscope (Shimadzu, UV-1280). Meanwhile, the functional groups as well as the chemical bonding of P-CQDs were recorded through FTIR with Attenuated Total Reflection (Shimadzu, IR Tracer-100). The fluorescent emission of P-CQDs was examined visually under UV light exposure (365 nm wavelength), confirming the formation of CQDs and their photoluminescent property (Jiang *et al.*, 2019, Kailasa *et al.*, 2019).

3. Results and Discussion

3.1 Banana Peel Powder Characteristics

The proximate analysis of the Cavendish BPP is summarized in Table 2. This was conducted using the Association of Official Agricultural Chemists (AOAC) analytical procedure (AOAC, 2016). The ash content observed at $13.35 \pm 0.22\%$ could be attributed to the mineral content such as calcium, potassium, and iron (Feumba *et al.*, 2016). The banana peel powder also contains lipids, which might be the saturated and unsaturated fatty acids present; as well as crude protein, which is linked to its naturally occuring amino acids (Happi Emaga *et al.*, 2007). Meanwhile, the moisture content of the raw banana peels was $88.92 \pm 3.35\%$ (w/w), which is consistent with the $89.68 \pm$

Table 2Proximate Composition of Cavendish Banana Peel Powder (g/100g)

(8, 1008)		
Composition	Amount	
Moisture	15.67 ± 0.15	
Crude Proteins	7.59 ± 0.31	
Lipids	3.81 ± 0.12	
Ash	13.35 ± 0.22	
Carbohydrates (by difference)	59.58 ± 7.43	

0.115% observed by Gomez-Montaño *et al.* (2021). While hydrothermal synthesis can handle this moisture level, drying and powdering the banana peels was preferred to accurately control the reaction medium and maintain the homogeneity of the carbon precursor. After pretreatment, the moisture content was reduced to 15.67 \pm 0.15% (w/w). Although this is slightly higher than the values reported in other studies, the carbohydrate content, approximately 59.58 \pm 7.43% remains consistent with previous findings (Gomez-Montaño *et al.*, 2020; Segura-Badilla *et al.*, 2022). This high carbohydrate content confirms that banana peels are rich in carbon, making them a viable precursor for synthesizing carbon quantum dots.

The FTIR spectrum of the banana peel powder, presented in Figure 2, reveals several key peaks. The wide band at 3281 cm⁻¹ corresponds to intense hydroxyl stretching vibration, while the absorption bands at 2918 cm⁻¹ and 2851 cm⁻¹ correspond to C-H stretching frequencies in the molecular backbone ascribed to the lipid compounds and some lignin fractions of the BPP (Oleveira et al., 2016). The aromatic stretching of the lignin fractions (Mohd Salim et al., 2015; Oleivera et al., 2016) is also reflected by the stretching signals of C=C vibrations at 1593 cm-1. Meanwhile, certain absorption bands are linked to cellulose and hemicellulose, such as the 1315 cm⁻¹ peak, which correponds to the to stretching of the C-H group, and the band at 1732 cm⁻¹, which is assigned to the C=O stretching of ester or carboxylic groups (Oleivera et al., 2016). A peak at 1024 cm⁻¹ ¹ is likely due to the C-O stretching frequencies of ester or ether functionalities, while a small peak at 889 cm⁻¹ may indicate N-H bending vibrations from amine groups (Memon et al., 2008). The findings above suggest that the banana peel powder contains phenol/alcohol, carboxyl, carbonyl, alkane, amine, and aromatic groups which are consistent with the proximate analytical results (Table 2). Furthermore, the presence of a strong hydroxyl group, indicates that banana peels are a precursor rich in cellulose, hemicellulose, and lignin (Oleivera et al., 2016).

3.2 P-CQDs Formation via Hydrothermal Synthesis

The reaction of the phosphoric acid with the abovementioned lignocellulosic components of the banana peel powder is essential in hydrothermal synthesis. During the process, phosphoric acid plays multiple roles not only serving as a doping agent but also acting as a catalyst. It facilitates the cleavage or scission of aryl ether linkages of the lignin groups in banana peel powder (Liu *et al.*, 2021). This catalytic action is

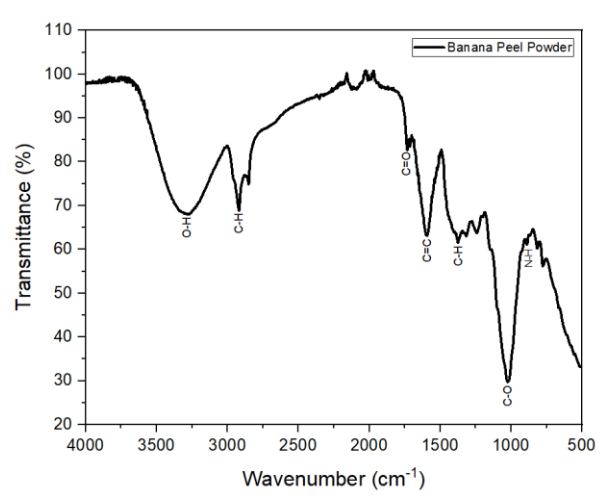


Fig. 2 FTIR Spectrum of Banana Peel Powder

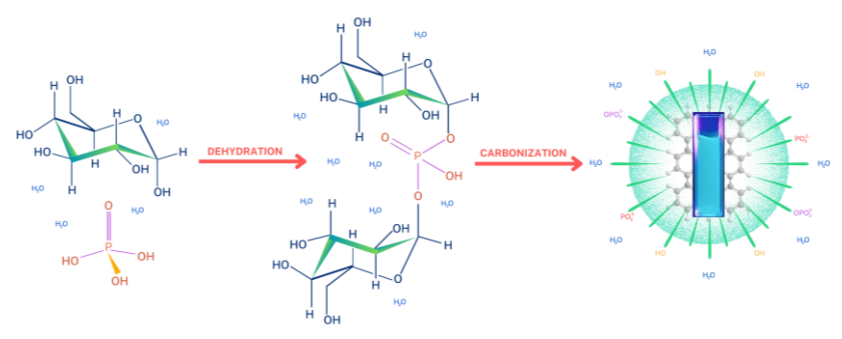


Fig. 3 Schematic Illustration of the Formation of P-CQDs

crucial as it drives the dehydration reaction, which plays the key role in the activation pathway (Goswami et al., 2022). Additionally, phosphoric acid has the ability to dehydrate hemicellulose, cellulose and lignin present in the BPP and it also functions as a crosslinker (in the form of phosphates or polyphosphates) to biopolymer fragments (Jagtoyen et al., 1998; Yakout et al., 2011). Furthermore, the low pH resulting from the addition of phosphoric acid stimulates the breakdown of hemicellulose and cellulose into furfural derivatives (Quesada-Plata et al., 2016). As the process continues, these furfural derivatives undergo polymerization, followed by aromatization and passivation during carbonization, which occurs through thermal decomposition (Goswami et al., 2022). This sequence of reactions ultimately leads to the formation of P-CQDs as illustrated in Figure 3. Surface oxidation during this process can also result in the formation of various acidic surface organic moieties including those containing phosphorus which was further confirmed by the FTIR analysis of the P-CQDs unveiled in the following discussion. These functional groups create active sites that can enhance the photocatalytic and electronic applications of the carbon nanomaterial (Liu et al., 2021).

3.3 Statistical Results and Effect of Factors

The model equation (Equation 1) predicts the photoreduction efficiency based on factorial levels. Note that the coefficients of the model below are scaled to acommodate the units of each factor and that the intercept is not at the center of the design space (Stat-Ease Inc., 2018).

$$PE = 145.4313 - 5.9375A - 0.3541B - 1.3969C$$
 (1)

where: PE is the photoreduction efficiency (%), A is H_3PO_4 :BPP mass ratio, B is the reaction temperature (°C), and C represents the reaction time (h).

The statistical data summarized in Table 3 showing ANOVA results at a 95% confidence interval confirms the statistical significance of the factorial model (p-value < 0.05). This suggests that it accounts for a significant portion of the variability in the photocatalytic reduction efficiency of hexavalent chromium. All three studied factors, phosphoric acid: banana peel powder mass ratio [A], reaction temperature [B], and reaction time [C] are highly significant, demonstrating their strong influence on the response variable. The significant curvature suggests the presence of an optimum level for one or more factors, which warrants further investigations through surface plots. Insignificant lack of fit shows that the model adequately fits the data with a coefficient of determination (R2) of 0.9580. The residual variance of 46.80 implies that a relatively small percentage of the total variability in the data is unexplained by the model. Meanwhile, the pure error of 32.36 represents the variability due to experimental error, reflecting good precision in replicate measurements. Based on the data, the mean square error of the pure error is slightly less than the residual mean square, indicating that most of the residual variance might be due to true variation rather than lack of model fit. Overall, this parametric analysis provides a comprehensive understanding of photoreduction efficiency, highlighting areas for optimizations, and confirming the robustness of the experimental model (Stat-Ease Inc., 2018).

3.3.1 Effect of Phosphoric Acid: Banana Peel Powder Mass Ratio

Increasing the amount of phosphoric acid appears to decrease photoreduction efficiency as illustrated in Figure 4a. Although phosphorus doping can enhance photocatalytic performance (Bhati *et al.*, 2019; Saini *et al.*, 2021), excessive phosphoric acid might create a harsh environment that may not be conducive to effective doping. The excessive concentration of H₃PO₄ in this

Table 3

Analysis of Variance (ANOVA) for Selected Factorial Model with Photoreduction Efficiency as a Response Variable

Sources	Sum of Square	Degrees of Freedom	Mean Square	F-value	p-value	Remarks
Model	1068.20	3	356.07	114.13	< 0.0001	Significant
[A]	141.02	1	141.02	45.20	< 0.0001	Significant
[B]	802.31	1	802.31	257.16	< 0.0001	Significant
[C]	124.88	1	124.88	40.03	< 0.0001	Significant
Curvature	29.89	1	29.89	9.58	0.0074	Significant
Residual	46.80	15	3.12			
Lack of Fit	14.44	4	3.61	1.23	0.3543	Not
Pure Error	32.36	11	2.94			Significant
Cor Total	1144.89	19				

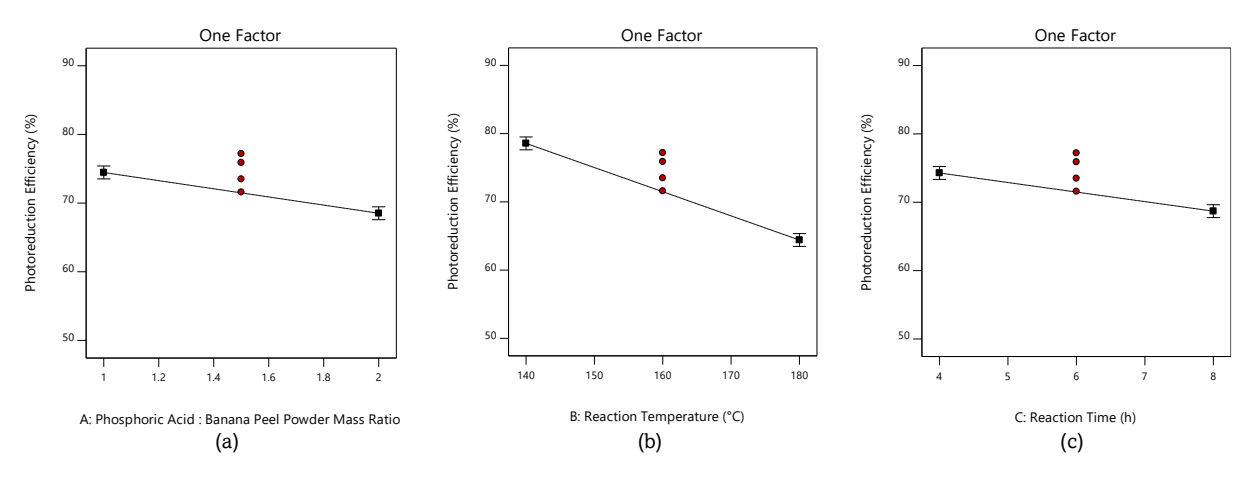


Fig. 4 Effect of Varying Hydrothermal Synthesis Condition on the Photocatalytic Reduction of Hexavalent Chromium

study seems to be unfavorable conditions for photocatalytic performance probably because of the high phosphorus-tocarbon ratio in the system. As shown in UV-vis spectra (Figure 6), introducing phosphoric acid can cause a redshift (bathochromic) in the absorbance band commonly observed when increasing the amount of nitrogen group elements like phosphorus, which can result in desirable energy transitions for P-CQD photocatalysts (Li et al., 2014; Kalaiyarasan et al., 2017; Kailasa et al., 2019). Nevertheless, further increasing the phosphorous group content might also lead to a loss of surfaceoxygen present on the carbonaceous product (Yakout et al., 2011). This decrease in oxygen-containing surface functional groups like the carbonyl, hydroxyl and carboxyl can result in fewer electrons for reducing the valency of the chromium (Chen et al., 2018). Hence, phosphoric acid optimal amount must be determined to ensure effective doping or passivation while avoiding conditions that could negatively affect the CQDs properties (Zhang et al., 2021).

3.3.2 Effect of Reaction Temperature

The hydrothermal reaction temperature has the highest effect on the photocatalytic performance of P-CQDs toward hexavalent chromium reduction. As shown in Figure 4b, increasing the synthesis temperature from 140°C to 180°C leads to a decline photocatalytic performance. This trend can be linked to the synthesis mechanism, where moderate heating facilitates better integration of dopants and passivating agents, despite higher temperatures potentially improving carbonization. P-CQDs synthesized at lower temperatures consistently perform better in the photoreduction of 50ppm hexavalent chromium, likely due to more effective phosphorus doping, which enhances visible light absorption through the quantum confinement effect and enhances the dissociation of photoinduced charge carriers (Liu et al., 2021). Furthermore, lower temperatures may result in highly passivated P-CQDs, whereas high temperatures can cause poor passivation (Omer et al., 2017; Azami et al., 2023). Meanwhile, elevated temperatures as high as 180°C to 200°C can degrade the doping agent, and promote agglomeration, which may reduce the effective surface area, thus lowering the photocatalytic performance (Zhang et al., 2021). A photocatalyst with a larger surface area is desirable since it has a higher number of active centers needed for producing more radical reactive species for effective photoreduction (Hassaan et al., 2023). Lower carbonization temperature may also result in higher presence of surface hydroxyl groups on the resulting carbon material while at high carbonization temperatures, the carbon might lack hydroxyl groups (Shu et al., 2024).

3.3.3 Effect of Reaction Time

Increasing the hydrothermal synthesis reaction time negatively impacts photoreduction efficiency as shown in Figure 4c. Extending the reaction time from 4 to 8 hours has minimal effect on photocatalytic performance, especially when compared to reaction temperature which affects the reduction profoundly. This suggests that the synthesis may have reached a saturation point where additional time does not enhance passivation or doping (Zhang et al., 2021). Similar to the effect of reaction temperature, longer reaction times result in less effective phosphorus doping on CQDs (Kalaiyarasan et al., 2020). Omer et al. (2017) also observed that longer heating times produced poorly passivated P-doped Carbon nanodots. UV-vis spectra (Figure 6) indicate that a broader peak at shorter wavelengths associated with the presence of the phosphorus group, is generally observed at shorter reaction times (Kalaiyarasan et al., 2020). Additionally, longer reaction times may lead to an extended nucleation phase, resulting in nanoparticle agglomeration (Prathumsuwan et al., 2018), which may reduce the surface sites, hence the amount of active centers for generating reactive oxygen species needed for hexavalent chromium reduction (Hassaan et al., 2023).

3.4 Photocatalytic Performance of P-CQDs

The photoreduction performance of P-CQDs towards 50ppm hexavalent chromium under 2 hours of visible light irradiation is in the range of 57.3% to 85.4%, as shown in Figure 5. P-CQDs synthesized under extreme conditions - high temperature (180 °C) extended reaction time (8 hours), and 2:1 phosphoric acid to banana peel powder mass ratio - exhibited the lowest photoreduction efficiency. Conversely, P-CQDs synthesized under milder conditions demonstrated the highest efficiency. These can be observed in the contour plots (Figures 5a and 5b) and the 3D surface plot (Figure 5c), where the red region (desirable region for photoreduction) lies on the milder conditions for each factor. This performance disparity can be attributed to the effectiveness of the doping process. As shown in the UV-Vis spectra in Figure 6, effective doping was observed at lower temperatures and reaction times. Similar findings were reported in a study using Trisodium citrate as the carbon source, where phosphorus doping in carbon quantum dots (CQDs) increases with rising temperatures up to 140°C, after which it decreases as the temperature continues to increase to 200°C

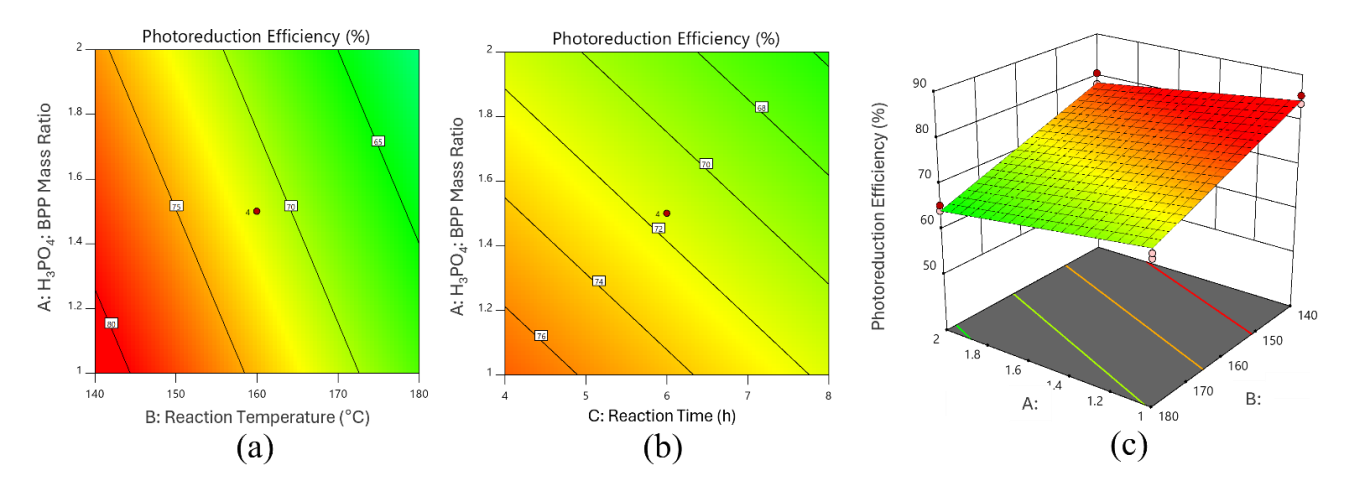


Fig. 5 Effect of Factorial Levels on the Photoreduction Efficiency (a,b) Contour Plots, and (c) 3D Surface Plot

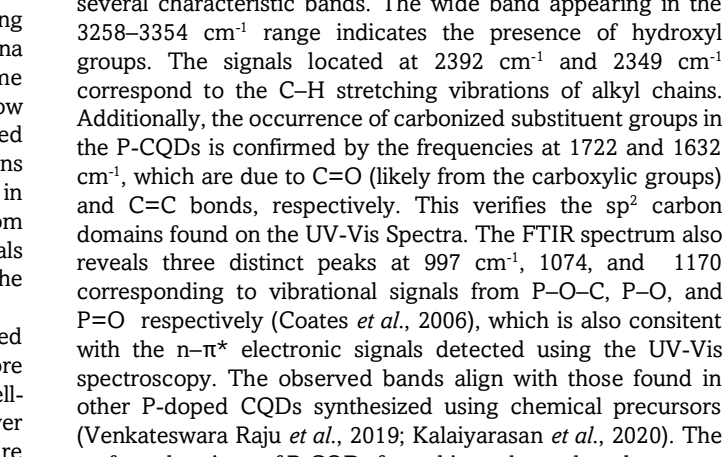
(Kalaiyarasan et al., 2020). This trend aligns with the reduction performance, where P-CQDs synthesized at lower temperatures outperformed those synthesized at higher temperatures (i.e., 180 °C). A similar pattern was observed for reaction time where P-CQDs synthesized at shorter durations showed better performance.

3.5 Characteristics of P-CQDs

3.5.1 UV-Visible Spectra

The UV-Vis spectrum of each P-CQD synthesized at varying hydrothermal synthesis conditions i.e., phosphoric acid: banana peel powder mass ratio, reaction temperature, and reaction time is given in Figure 6. It can be observed that P-CQDs show distinct peaks at a wavelength between 190 and 250 nm linked to π - π * transitions of the sp² carbon in the aromatic domains present in the inner core (Akbar et al., 2021). An increase in absorbance is also noticeable as the wavelength decreases from 350nm to 250nm which originates to the n- π * electronic signals primarily associated with C=P, C=O, and P=O bonds on the surface of the CQDs (Kalaiyarasan et al., 2020).

All P-CODs synthesized at 140°C exhibit a more defined peak on this wavelength range showing that doping is more effective at this temperature. General observation of the welldefined peaks of $n-\pi^*$ depicts better doping at lower temperature and shorter reaction time. These observations are



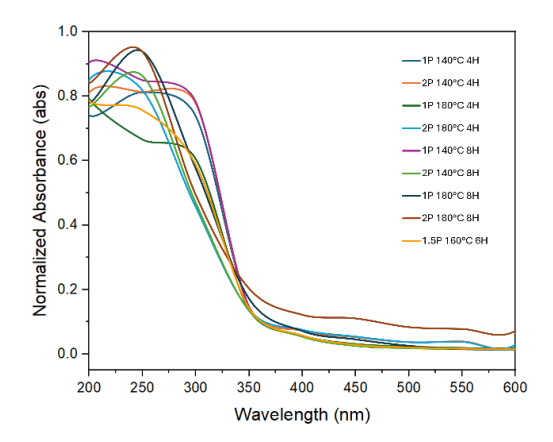


Fig. 6 UV-Vis Spectra of P-CQDs Synthesized at Varying Hydrothermal Conditions

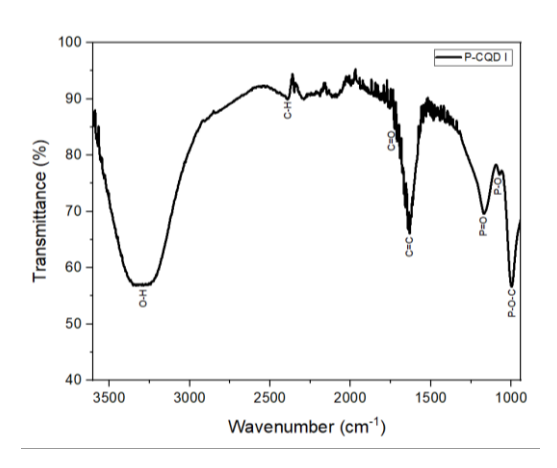


Fig. 7 FTIR Spectrum of P-CQD I

The FTIR spectrum of a representative sample, P-CQD I

3.5.2 FTIR Spectrum

(synthesized at 160°C, 6 hours reaction time, and 1.5 H₃PO₄: banana peel powder mass ratio) as shown in Figure 7, exhibits several characteristic bands. The wide band appearing in the surface chemistry of P-CQDs from this study renders them as n-

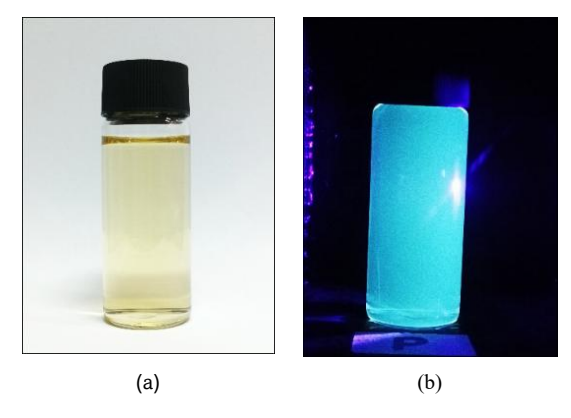


Fig. 8 P-CQD I Photographs under (a) Daylight (b) 365nm UV light

type moieties (electron donors), as they are capable of donating electrons to other substances like the hexavalent chromium (Azami *et al.*, 2023). In addition to acting as active centers for the production of reactive oxygen species during photoreduction, these surface traps also functions as electron scavengers, suppressing the electron and hole recombination and facilitating efficient charge transfer (Das *et al.*, 2021). Likewise, carbonyl, carboxyl, and phosphate groups may enhance the aqueous solubility and stability of the carbon nanomaterial (Atchudan *et al.*, 2020; Goswami *et al.*, 2022).

3.5.3 Fluorescent Property

In this study, P-CQDs synthesized via the hydrothermal method exhibited a yellow color under daylight and blue-green emission upon excitation with 365nm UV light, as represented in Figure 8a and Figure 8b, respectively. As confirmed in the UV-Vis and FTIR Spectra, sp²-hybridized carbon core are present in the P-CQDs, characterizing the formation of π -domains during the synthesis process. The observed fluorescence may be attributed to the carbon core state emissions, resulting from the radiative transitions across the energy band within the internal π -region, likely influenced by the quantum confinement effect (Alafeef et al., 2024). In phosphorus-rich CQDs, fluorescence could also be affected by the ability of the phosphorus to penetrate the carbogenic core of the CQDs (Azami et al., 2023). Additionally, the photoluminescence of the P-CQDs may also be credited to surface defects or states (Papaioannou et al., 2019), which can be described as a boundary regions surrounding the C=C core (Alafeef et al., 2024). As depicted in Figure 7, the synthesized P-CQDs contain functional groups that predominantly contain oxygen, which could increase surface defects and, in turn, create more emission sites (Jiang et al., 2019). However, the molecular state theory, which is common in low-temperature bottom-up approaches like hydrothermal process, can also be considered. It is possible that during synthesis, fragments of fluorophore molecules derived from the feed materials are either distributed on the surface of the dots or integated into the carbon core (Alafeef et al., 2024). Although this study did not specifically investigate the fluorescence mechanism nor the presence of fluorophores during the hydrothermal processing of banana peel powder, the exact contributions of these factors to the observed fluorescence require further investigation.

4. Conclusion

This research effectively produced P-CQDs from banana peels and phosphoric acid through a hydrothermal approach. The UV-Vis spectroscopy confirmed the formation of P-CQDs, indicated by the $\pi-\pi^*$ transitions of the sp^2 carbon in the core and the $n-\pi^*$ domains primarily linked with C=O, C=P, and P=O bonds on the CQD surface. FTIR analysis further revealed characteristic bands corresponding to hydroxyl, carbonyl, carboxyl, and phosphorous-containing functional groups, which may act as active sites for generating reactive oxygen species responsible for photocatalysis under visible light irradiation. Another notable property of the synthesized compound is its strong photoluminescence with blue-green emissions under 365nm UV light, which supports its possible applications in bioimaging, fluorescent sensing, and anticounterfeiting.

This study demonstrated that the synthesized P-CQDs exhibited promising photocatalytic activity, with a reduction efficiency for 50 ppm Cr (VI) ranging from 57.3% to 85.4% under 2 hours of visible light irradiation. Statistical analysis of the 2^k factorial experiment confirmed the significant effect of varying hydrothermal conditions such as phosphoric acid to banana peel powder mass ratio, reaction temperature, and reaction time on the performance of P-CQDs in photoreduction. Overall, this study highlights the potential of utilizing green sources, like banana peels, for the sustainable fabrication of photocatalysts for environmental remediation. Furthermore, the performance of the synthesized photocatalysts under visible light opens new possibilities for sunlight-driven photocatalysis and in solar energy harnessing and development.

Acknowledgments

I gratefully acknowledge the financial support from the Department of Science and Technology – Engineering Research and Development for Technology (DOST-ERDT) for this research, as well as the technical assistance provided by Mach Union Laboratories, Incorporated. I am also profoundly thankful to my mentors, and my parents, Mr. Alfredo Asi Claus and Mrs. Yolanda Bool Marasigan—Claus, for their unwavering support.

Author Contributions: C.M.C.: conceptualization, methodology, formal analysis, writing—original draft; M.C.M.D: supervision, resources, formal analysis, writing—review and editing; J.A.C.: writing—review and editing; R.B.C.: writing—review and editing; M.C.dB.: writing—review and editing. All authors have read and agreed to the published version of the manuscript.

Funding: This research was funded by Department of Science and Technology – Engineering Research and Development for Technology (DOST-ERDT).

Conflicts of Interest: The authors declare no conflict of interest.

References

Ahmed, Z., El-Sharnouby, G., & El-Waseif, M. (2021). Use of Banana Peel As A By-Product to Increase The Nutritive Value of The Cake. *Journal of Food and Dairy Sciences*, 12(4), 87-97. https://doi.org/10.21608/jfds.2021.167053

Akbar, K., Moretti, E., & Vomiero, A. (2021). Carbon Dots for Photocatalytic Degradation of Aqueous Pollutants: Recent Advancements. *Advanced Optical Materials*, 9(17), 2100532. https://doi.org/10.1002/adom.202100532

Alafeef, M., Srivastava, I., Adutya, T., & Pan,D. (2024). Carbon Dots: From Synthesis to Unraveling the Fluorescence Mechanism. Small, 20(4), 2303937. https://doi.org/10.1002/smll.202303937

Alkian, I., Sutanto, I., Hadiyanto, H. (2022). Quantum yield optimization of carbon dots using response surface methodology and its

- application as control of Fe3+ion levels in drinking water. Mater. Res. Express 9 015702. https://doi.org/10.1088/2053-1591/ac3f60
- Alzate Acevedo, S., Díaz Carrillo, Á. J., Flórez-López, E., & Grande-Tovar, C. D. (2021). Recovery of Banana Waste-Loss from Production and Processing: A Contribution to a Circular Economy. *Molecules*, 26(17), 5282. https://doi.org/10.3390/molecules26175282
- AOAC Association of Official Agricultural Chemists (2016). Official Methods of Analysis. 16th ed.
- Atchudan, R., Edison, T. N. J. I., Perumal, S., Vinodh, R., Sundramoorthy, A. K., Babu, R. S., & Lee, Y. R. (2021). Leftover Kiwi Fruit Peel-Derived Carbon Dots as a Highly Selective Fluorescent Sensor for Detection of Ferric Ion. *Chemosensors*, 9(7), 166. https://doi.org/10.3390/chemosensors9070166
- Atchudan, R., Jebakumar Immanuel Edison, T. N., Shanmugam, M., Perumal, S., Somanathan, T., & Lee, Y. R. (2020). Sustainable synthesis of carbon quantum dots from banana peel waste using hydrothermal process for in vivo bioimaging. *Physica E: Low-Dimensional Systems and Nanostructures*, 114417. https://doi.org/10.1016/j.physe.2020.114417
- ATSDR Agency for Toxic Substances and Disease Registry (2000).

 Toxicological Profile for Chromium. U.S. Department of Health and Human Services, Public Health Service. https://www.atsdr.cdc.gov/toxprofiles/tp7.pdf
- Azami, M., Wei, J., Valizadehderakhshan, M., Jayapalan, A., & Ayodele, O. O. (2023). Effect of Doping Heteroatoms on the Optical Behaviors and Radical Scavenging Properties of Carbon Nanodots. *The Journal of Physical Chemistry C*, 127(23), 10178-10190. https://doi.org/10.1021/acs.jpcc.3c00953
- Baird, R., & Bridgewater, L. (2017). Standard methods for the examination of water and wastewater. 23rd edition. Washington, D.C., American Public Health Association.
- Bhati, A., Anand, S. R., Saini, D., Gunture, & Sonkar, S. K. (2019). Sunlight-induced photoreduction of Cr(VI) to Cr(III) in wastewater by nitrogen-phosphorus-doped carbon dots. *Npj Clean Water*, 2(1). https://doi.org/10.1038/s41545-019-0036-z
- Burstein, G. T. (2010). Passivity and Localized Corrosion. *Shreir's Corrosion*, 2, 731–752. https://doi.org/10.1016/b978-044452787-5.00198-0
- Cai, Z., Li, F., Rong, M., Lin, L., Yao, Q., Huang, Y., Wang, X. (2019). Introduction. *Novel Nanomaterials for Biomedical, Environmental and Energy Applications*, 1–36. https://doi.org/10.1016/b978-0-12-814497-8.00001-1
- Carbonaro, Corpino, Salis, Mocci, Thakkar, Olla, & Ricci. (2019). On the Emission of Carbon Dots: Reviewing Data and Discussing Models. *C Journal of Carbon Research*, 5(4), 60. https://doi.org/10.3390/c5040060
- Çetin, D., Dönmez, S., & Dönmez, G. (2008). The treatment of textile wastewater including chromium(VI) and reactive dye by sulfate-reducing bacterial enrichment. *Journal of Environmental Management*, 88(1), 76–82. https://doi.org/10.1016/j.jenvman.2007.01.019
- Chen, Y., An, D., Sun, S., Gao, J., & Qian, L. (2018). Reduction and Removal of Chromium VI in Water by Powdered Activated Carbon. *Materials*, 11(2), 269. https://doi.org/10.3390/ma11020269
- Coates, J. (2006). Interpretation of Infrared Spectra, A Practical Approach. *Encyclopedia of Analytical Chemistry*. https://doi.org/10.1002/9780470027318.a5606
- DA-Department of Agriculture (2018). Philippine Banana Industry Roadmap 2019-2022. https://www.da.gov.ph/wp-content/uploads/2019/06/Philippine-Banana-Industry-Roadmap-2019-2022.pdf
- Das, S., Ngashangva, L., & Goswami, P. (2021). Carbon Dots: An Emerging Smart Material for Analytical Applications. *Micromachines*, 12(1), 84. https://doi.org/10.3390/mi12010084
- Dastgheib, S. A., & Rockstraw, D. A. (2001). Pecan Shell Activated Carbon: Synthesis, Characterization, and Application for the Removal of Copper from Aqueous Solution. *Carbon*, 39(12), 1849– 1855. https://doi.org/10.1016/s0008-6223(00)00315-8
- FAO UN Food and Agriculture Organization of the United Nations (2022). Banana Market Review 2021. Rome. https://www.fao.org/3/cc1610en/cc1610en.pdf

- Feumba, D.R., Ashwini R.P., & Ragu, S.M. (2016). Chemical Composition of Some Selected Fruit Peels. *European Journal of Food Science and Technology*, 4(4). 12-21. https://www.researchgate.net/publication/326579276_Chemic al composition of some selected fruit peels
- Gomez-Montaño, F. J., Bolado-Garcia, V.E., & Blasco-Lopez, G. (2020). Compositional and antioxidant analysis of peels from different banana varieties (*Musa spp.*) for their possible use in developing enriched flours. *Acta Universitaria*, 29, e2260. https://doi.org/10.15174/au.2019.2260
- Goswami, J.Rohman, S., Guha, A. Basyach, P., Sonowal, K., Borah, S., & Saikia, L., & Hazarika, P. (2022). Phosphoric acid assisted synthesis of fluorescent carbon dots from waste biomass for detection of Cr(VI) in aqueous media. *Materials Chemistry and Physics*. 286. 126133. https://doi.org/10.1016/j.matchemphys.2022.126133
- Happi Emaga, T., Andrianaivo, R. H., Wathelet, B., Tchango, J. T., & Paquot, M. (2007). Effects of the stage of maturation and varieties on the chemical composition of banana and plantain peels. *Food Chemistry*, 103(2), 590–600. https://doi.org/10.1016/j.foodchem.2006.09.006
- Hassaan, M. A., El-Nemr, M. A., Elkatory, M. R., & El-Din, G. T. (2023).
 Principles of Photocatalysts and Their Different Applications: A Review. Topics in Current Chemistry, 381(1), 31.
 https://doi.org/10.1007/s41061-023-00444-7
- Hoang, A.T., Pandey, A., Chen, W.H., Ahmed, S.F., Nizetic, S., Ng, K.H., Said, Z., Duong, X.Q., Agbulut, U., (2023). Hadiyanto, H.; Hydrogen Production by Water Splitting with Support of Metal and Carbon-Based Photocatalysts. ACS Sustainable Chem. Eng. 11(4), 1221–1252
- Jagtoyen, M., & Derbyshire, F. (1998). Activated Carbons from Yellow Poplar and White Oak by H₃PO₄ Activation. *Carbon*, 36(7-8), 1085–1097. https://doi.org/10.1016/s0008-6223(98)00082-7
- Jiang, K., Feng, X., Gao, X., Wang, Y., Cai, C., Li, Z., & Lin, H. (2019).
 Preparation of Multicolor Photoluminescent Carbon Dots by Tuning Surface States. *Nanomaterials*, 9(4), 529.
 https://doi.org/10.3390/nano9040529
- John, V. L., Nair, Y., & Vinod, T. P. (2021). Doping and Surface Modification of Carbon Quantum Dots for Enhanced Functionalities and Related Applications. *Particle & Particle Systems Characterization*, 38(11), 2100170. https://doi.org/10.1002/ppsc.202100170
- Kailasa, S. K., Ha, S., Baek, S. H., Phan, L. M. T., Kim, S., Kwak, K., & Park, T. J. (2019). Tuning of carbon dots emission color for sensing of Fe³⁺ ion and bioimaging applications. Materials Science and Engineering: C, 98, 834–842. https://doi.org/10.1016/j.msec.2019.01.002
- Kalaiyarasan, G., & Joseph, J. (2017). Determination of Vitamin B12 via pH-Dependent Quenching of the Fluorescence of Nitrogen-Doped Carbon Quantum Dots. *Microchimica Acta*, 184(10), 2017, 3883–3891. https://doi.org/10.1007/s00604-017-2421-y
- Kalaiyarasan, G., Joseph, J., & Kumar, P. (2020). Phosphorus-Doped Carbon Quantum Dots as Fluorometric Probes for Iron Detection. *ACS Omega*, 5 (35), 22278-22288. https://doi.org/10.1021/acsomega.0c02627
- Kropschot, S.J., & Doebrich, J. (2010). Chromium—Makes Stainless Steel Stainless. U.S. Geological Survey-Fact Sheet, 3089, 2. https://doi.org/10.3133/fs20103089
- Li, X., Zhang, S., Kulinich, S. A., Liu, Y., & Zeng, H. (2014). Engineering Surface States of Carbon Dots to Achieve Controllable Luminescence for Solid-Luminescent Composites and Sensitive Be²⁺ Detection. *Scientific Reports*, 4(1). https://doi.org/10.1038/srep04976
- Liu, W., Ning, C., Sang, R., Hou, Q., & Ni, Y. (2021). Lignin-derived graphene quantum dots from phosphorus acid-assisted hydrothermal pretreatment and their application in photocatalysis. *Industrial Crops and Products*, 171, 113963. https://doi.org/10.1016/j.indcrop.2021.113963
- Marqués, M. J., Salvador, A., Morales-Rubio, A. E., & de la Guardia, M. (1998). Analytical methodologies for chromium speciation in solid matrices: a survey of literature. *Fresenius' Journal of Analytical Chemistry*, 362(3), 239–248. https://doi.org/10.1007/s002160051067

- Memon, J. R., Memon, S. Q., Bhanger, M. I., Memon, G. Z., El-Turki, A., & Allen, G. C. (2008). Characterization of Banana Peel by Scanning Electron Microscopy and FT-IR Spectroscopy and Its Use for Cadmium Removal. *Colloids and Surfaces B: Biointerfaces*, 66(2), 2008. 260–265. https://doi.org/10.1016/j.colsurfb.2008.07.001
- Mohd Salim, R., Khan Chowdhury, A. J., Rayathulhan, R., Yunus, K., & Sarkar, Md. Z. I. (2015). Biosorption of Pb and Cu from Aqueous Solution Using Banana Peel Powder. *Desalination and Water Treatment*, 57(1), 303–314. https://doi.org/10.1080/19443994.2015.1091613
- Muktha, H., Sharath, R., Kottam, N., Smrithi, S. P., Samrat, K., & Ankitha, P. (2020). Green Synthesis of Carbon Dots and Evaluation of Its Pharmacological Activities. *BioNanoScience*, 10, 731–744. https://doi.org/10.1007/s12668-020-00741-1
- Oliveira, T. Í. S., Rosa, M. F., Cavalcante, F. L., Pereira, P. H. F., Moates, G. K., Wellner, N., Azeredo, H. M. C. (2016). Optimization of pectin extraction from banana peels with citric acid by using response surface methodology. *Food Chemistry*, 198, 113–118. https://doi.org/10.1016/j.foodchem.2015.08.080
- Omar, N. A. S., Fen, Y. W., Irmawati, R., Hashim, H. S., Ramdzan, N. S. M., & Fauzi, N. I. M. (2022). A Review on Carbon Dots: Synthesis, Characterization and Its Application in Optical Sensor for Environmental Monitoring. *Nanomaterials*, 12(14), 2365. https://doi.org/10.3390/nano12142365 nano12142365
- Omer, K. M., & Hassan, A. Q. (2017). Chelation-Enhanced Fluorescence of Phosphorus Doped Carbon Nanodots for Multi-Ion Detection. *Microchimica Acta*, 184(7), 2017, 2063–2071. https://doi.org/10.1007/s00604-017-2196-1
- Omm-e-Hany, Asia, N., Aamir, A., & Humaira, K. (2018) Determination of chromium in the tannery wastewater, Korangi, Karachi. *International Journal of Environmental Sciences & Natural Resources*, 15(4), 555920. https://doi.org/10.19080/IJESNR.2018.15.555920
- Papaioannou, N., Titirici, M.M., & Sapelkin, A. (2019). Investigating the Effect of Reaction Time on Carbon Dot Formation, Structure, and Optical Properties. *ACS Omega*, 4(26), 21658–21665. https://doi.org/10.1021/acsomega.9b01798
- Peralta-Videa, J. R., Zhao, L., Lopez-Moreno, M. L., de la Rosa, G., Hong, J., & Gardea-Torresdey, J. L. (2011). Nanomaterials and the environment: A review for the biennium 2008–2010. *Journal of Hazardous Materials*, 186(1), 1–15. https://doi.org/10.1016/j.jhazmat.2010.11.020
- Prathumsuwan, T., Jamnongsong, S., Sampattavanich, S., & Paoprasert, P. (2018). Preparation of carbon dots from succinic acid and glycerol as ferrous ion and hydrogen peroxide dual-mode sensors and for cell imaging. *Optical Materials*, 86, 517–529. https://doi.org/10.1016/j.optmat.2018.10.054
- Quesada-Plata, F., Ruiz-Rosas, R., Morallón, E., & Cazorla-Amorós, D. (2016). Activated Carbons Prepared through H3PO4-Assisted Hydrothermal Carbonisation from Biomass Wastes: Porous Texture and Electrochemical Performance. *ChemPlusChem*, 81(12), 1349–1359. https://doi.org/10.1002/cplu.201600412
- Rahim, S., Radiman, S., & Hamzah, A. (2012). Inactivation of Escherichia coli Under Fluorescent Lamp using TiO₂ Nanoparticles Synthesized Via Sol-Gel Method. *Sains Malaysiana*. 41, 219-224. https://www.researchgate.net/publication/263848400_Inactivation_of_Escherichia_coli_Under_Fluorescent_Lamp_using_TiO_2_Nanoparticles_Synthesized_Via_Sol_Gel_Method
- Ramar, V., Moothattu, S., & Balasubramanian, K. (2018). Metal free, sunlight and white light based photocatalysis using carbon quantum dots from Citrus grandis: A green way to remove pollution. Solar Energy, 169, 120–127. https://doi.org/10.1016/j.solener.2018.04.040
- Sa'adah, F., Sutanto, H., Hadiyanto, H., & Alkian, I. (2024). Efficient removal of amoxicillin, ciprofloxacin, and tetracycline from aqueous solution by Cu-Bi2O3 synthesized using precipitation-assisted-microwave. Communications in Science and Technology, 9(1), 170-178. https://doi.org/10.21924/cst.9.1.2024.1444
- Saini, D., Aggarwal, R., Sonker, A. K., & Sonkar, S. K. (2021). Photodegradation of Azo Dyes in Sunlight Promoted by Nitrogen–Sulfur–Phosphorus Codoped Carbon Dots. ACS Applied

- Nano Materials, 4(9), 9303–9312. https://doi.org/10.1021/acsanm.1c01810
- Segura-Badilla, O., Kammar-García, A., Mosso-Vázquez, J., Sánchez, R.A., Ochoa-Velasco, C., Hernández-Carranza, P., & Navarro-Cruz, A.R. (2022). Potential use of banana peel (*Musa cavendish*) as ingredient for pasta and bakery products. *Heliyon*, 8(10), e11044. https://doi.org/10.1016/j.heliyon.2022.e11044
- Shen, L., Liang, S., Wu, W., Liang, R., & Wu, L. (2013). Multifunctional NH₂-mediated zirconium metal–organic framework as an efficient visible-light-driven photocatalyst for selective oxidation of alcohols and reduction of aqueous Cr(VI). *Dalton Transactions*, 42(37), 13649. https://doi.org/10.1039/c3dt51479j
- Shu, D., Zhang, J., Ruan, R., Lei, H., Wang, Y., Moriko, Q., Zou, R., Huo, E., Duan, D., Gan, L., Zhou, D., Zhao, Y., & Dai, L. (2024). Insights into Preparation Methods and Functions of Carbon-Based Solid Acids. *Molecules*, 29(1), 247. https://doi.org/10.3390/molecules29010247
- Stat-Ease Inc. (2018). Design-Expert Software Documentation (Version 11)
- Sukmana, H., Bellahsen, N., Pantoja, F., & Hodur, C. (2021). Adsorption and coagulation in wastewater treatment Review. *Progress in Agricultural Engineering Sciences*, 17(1), 49–68. https://doi.org/10.1556/446.2021.00029
- Tchounwou, P. B., Yedjou, C. G., Patlolla, A. K., & Sutton, D. J. (2012).

 Heavy Metal Toxicity and the Environment. *Molecular, Clinical and Environmental Toxicology*, 101, 133–164. https://doi.org/10.1007/978-3-7643-8340-4_6
- Teh, C. Y., Budiman, P. M., Shak, K. P. Y., & Wu, T. Y. (2016). Recent Advancement of Coagulation–Flocculation and Its Application in Wastewater Treatment. *Industrial & Engineering Chemistry Research*, 55(16), 4363–4389. https://doi.org/10.1021/acs.iecr.5b04703
- Tungare, K., Bhori, M., Racherla, K. S., & Sawant, S. (2020). Synthesis, characterization and biocompatibility studies of carbon quantum dots from *Phoenix dactylifera*. *3 Biotech*, 10(12), 540. https://doi.org/10.1007/s13205-020-02518-5
- Venkateswara Raju, C., Kalaiyarasan, G., Paramasivam, S., Joseph, J., & Senthil Kumar,S. (2019). Phosphorous Doped Carbon Quantum Dots as an Efficient Solid State Electrochemiluminescence Platform for Highly Sensitive Turn-On Detection of Cu²⁺ Ions. *Electrochimica Acta*, 135391. https://doi.org/10.1016/j.electacta.2019.135391
- Vikneswaran, R., Ramesh, S., & Yahya, R. (2014). Green synthesized carbon nanodots as a fluorescent probe for selective and sensitive detection of Iron(III) ions. Materials Letters, 136, 179–182. https://doi.org/10.1016/j.matlet.2014.08.063
- Wang. C., Shi H., Yang, M., Yao, Z, Zhang, B., Liu, E., Hu, X., Xue, W., & Fan., J. (2021). Biocompatible sulfur nitrogen co-doped carbon quantum dots for highly sensitive and selective detection of dopamine. *Colloids and Surfaces B: Biointerfaces*, 205, 111874. https://doi.org/10.1016/j.colsurfb.2021.111874
- Wilbur, S., Abadin, H., & Fay, M. (2012). Toxicological Profile for Chromium. *Atlanta (GA): Agency for Toxic Substances and Disease Registry (US)*. Production, Import/Export, Use, and Disposal. https://www.ncbi.nlm.nih.gov/books/NBK158858/
- Xia, C., Zhu, S., Feng, T., Yang, M., & Yang, B. (2019). Evolution and Synthesis of Carbon Dots: From Carbon Dots to Carbonized Polymer Dots. Advanced Science, 6(23),1901316. https://doi.org/10.1002/advs.201901316
- Xu, L., Bai, X., Guo, L., Yang, S., Jin, P., & Yang, L. (2018). Facial fabrication of carbon quantum dots (CDs)-modified N-TiO₂-x nanocomposite for the efficient photoreduction of Cr(VI) under visible light. *Chemical Engineering Journal*, 357, 473-486. https://doi.org/10.1016/j.cej.2018.09.172
- Yakout, S. M., & Sharaf El-Deen, G. (2011). Characterization of Activated Carbon Prepared by Phosphoric Acid Activation of Olive Stones. *Arabian Journal of Chemistry*, 70 (S2), 2011. https://doi.org/10.1016/j.arabjc.2011.12.002
- Yli-Pentti, A. (2014). Electroplating and Electroless Plating. Comprehensive Materials Processing, 4, 277–306. https://doi.org/10.1016/b978-0-08-096532-1.00413-1
- Zhang, H., Wang, H., Wang, Y., & Xin, B. (2020). Controlled synthesis and photocatalytic performance of biocompatible uniform carbon quantum dots with microwave absorption capacity. *Applied*

Surface Science, 512, 145751. https://doi.org/10.1016/j.apsusc.2020.145751
Zhang, S.R., Cai, S.K., Wang, G.Q., Cui, J.Z., & Gao, C.Z. (2021). Onestep synthesis of N, P-doped carbon quantum dots for selective

and sensitive detection of Fe^{2+} and Fe^{3+} and scale inhibition. Journal of Molecular Structure, 1246, 131173. https://doi.org/10.1016/j.molstruc.2021.131173



© 2025. The Author(s). This article is an open access article distributed under the terms and conditions of the Creative Commons Attribution-ShareAlike 4.0 (CC BY-SA) International License (http://creativecommons.org/licenses/by-sa/4.0/)